


Combined Albumin Polyester Nanocarriers with Docetaxel for Effective Against Lung Cancer in Mice Model

Yixiao Yang^{1,*}, Tao Ye^{2,*}, Fusheng Shang³, Dagui Chen³, Kai Wang¹, Shengli He⁴

¹Research Center of Nanomedicine Technology, The Second Affiliated Hospital of Guangxi Medical University, Nanning, 530000, People's Republic of China; ²Department of Oncology, Minhang Branch, Zhongshan Hospital, Fudan University, Shanghai, 201100, People's Republic of China; ³Institute of Translational Medicine, Shanghai University, Shanghai, 200444, People's Republic of China; ⁴Department of Hepatobiliary-Pancreatic and Integrative Oncology, Minhang Branch, Fudan University Shanghai Cancer Center, Shanghai, 200240, People's Republic of China

*These authors contributed equally to this work

Correspondence: Kai Wang; Shengli He, Email kaiwang16@fudan.edu.cn; hlshli@yeah.net

Introduction: Lung cancer, a deadly malignancy, often employs Docetaxel (DTX) as a chemotherapy option. However, DTX non-selective distribution limits its therapeutic effectiveness due to adverse side effects. This study aims to develop novel folate-targeted albumin polyester nanocarriers (FA-DTX-APs) encapsulating DTX for precise delivery, enhancing lung cancer treatment efficacy.

Methods: FA-DTX-APs were meticulously crafted utilizing the thin-film dispersion technique and subsequently evaluated for their physicochemical characteristics, encapsulation efficiency, and drug release profiles. To assess their biological properties, anti-tumor efficacy, and biosafety in the context of lung cancer, a comprehensive series of hemolysis assays, cellular studies, and animal experiments were conducted.

Results: FA-DTX-APs exhibit nanovesicle properties with a size of (223.65 ± 6.83) nm, a potential of (26.76 ± 3.15) mV, and encapsulate DTX with high efficiency $(96.19 \pm 3.27\%)$ and loading capacity $(9.75 \pm 0.38\%)$. FA-DTX-APs enable tumor-targeted drug delivery and slow release of the drug over a long period of time, with faster release in acidic environments. By efficiently targeting and entering lung cancer cells, FA-DTX-APs effectively hinder cancer growth ($P < 0.05$), demonstrating superior anti-tumor effects ($P < 0.05$), biocompatibility and enhanced biological safety ($P < 0.05$).

Conclusion: This study introduces FA-DTX-APs, an innovative nanocarrier characterized by exceptional biocompatibility and safety. It successfully targets lung cancer cells to deliver DTX in a sustained, slow-release manner, ensuring prolonged tumor-killing effects. As such, FA-DTX-APs hold immense promise as a novel nanoagent for lung cancer therapy.

Keywords: lung cancer, Docetaxel, folate, albumin, polyester

Introduction

Lung cancer stands as one of the most prevalent forms of malignant tumors worldwide, accounting for approximately 2.2 million new cases and claiming 1.8 million lives annually.¹ Chemotherapy, a cornerstone in its treatment, is pervasively employed yet fraught with numerous detrimental side effects on patients' bodies, particularly due to the limitations imposed by the administration routes on the efficacy of chemotherapeutic agents.^{2,3} Among these agents, Docetaxel (DTX), a paclitaxel derivative, is a commonly prescribed drug for lung cancer treatment. However, its clinical performance is often hampered by non-selective distribution in the body, leading to undesired side effects.^{4,5} Thus, the crux of DTX-based lung cancer therapy lies in enhancing its concentration within lung tumor cells-achieving targeted delivery specifically to tumors. This strategy promises to maximize DTX's therapeutic potential while minimizing its toxicity and side effects in non-target tissues. In recent times, researchers have explored innovative DTX formulations, including nanoparticles,⁶ nanoliposomes,⁷ pH-sensitive liposomes,⁸ micelles,⁹ and microspheres,¹⁰ to address the challenges of inadequate tumor targeting, solvent burden, and excessive drug dosing in conventional formulations. While

these advancements have shown promise, they still grapple with significant limitations in optimizing DTX efficacy, mitigating toxic side effects, and facilitating large-scale production.^{11,12} Consequently, the development of novel DTX formulations that precisely target tumor sites holds immense significance, offering the potential to revolutionize lung cancer treatment by enhancing drug delivery precision and safety.

Recent years have witnessed the proliferation of biomaterials, particularly polymer-based organic polymers, in crafting nano drug carriers. These carriers offer superior molecular size control, enhanced permeability, and exceptional biocompatibility and degradability, making them a prime focus for anti-tumor drug carrier research.^{13,14} Among them, Polyethylene glycol (PEG) and Poly (L-lactide-co-glycolide) (PLGA) have secured FDA approval for clinical use.^{15,16} PEG, a versatile polymer carrier, can be easily tailored at its termini and integrated with hydrophobic polymers to form amphiphilic structures through block or graft polymerization, as well as surface functionalization, enabling active targeting in nanomedicine.^{15,16} PLGA, a biodegradable hydrophobic polymer derived from lactic and glycolic acids, degrades into harmless metabolites excreted naturally, ensuring non-toxicity and non-immunogenicity.^{15,16} By fusing PEG and PLGA, PEG-PLGA copolymer carriers overcome their individual limitations. Acting as a matrix, PEG-PLGA forms amphiphilic copolymer vesicles tailored to encapsulate drugs in either the hydrophobic shell or hydrophilic core. These vesicles exhibit remarkable hematological stability, biocompatibility, and controlled release properties, broadening their clinical applicability.^{15–17}

In recent years, albumin-based nanomaterials have been widely used in nanoparticle drug delivery systems due to their diverse properties. Bovine serum albumin (BSA) is favored among these developed materials as an endogenous protein with the following excellent properties:^{18,19} 1) it is the most abundant protein in plasma with good biocompatibility, biodegradability, and low toxicity; 2) it has many amino and carboxyl groups that can be used to link functional ligands; 3) there are 17 disulfide bonds within the BSA molecule, which allow loading of drugs by cross-linking the disulfide bonds; and 4) it has a half-life of up to 19 days. Albumin nanoparticles have attracted much attention in the delivery of antitumor drugs due to their great potential for drug loading and biomedical applications.¹⁸ These albumin-based nanoparticles show great advantages such as accumulating in tumor tissues through enhanced permeability and retention (EPR) effects, prolonging the blood circulation time of antitumor drugs, and exhibiting biocompatibility in vivo.^{20,21} However, problems such as poor tumor targeting and uncontrolled intracellular drug release of these albumin nanoparticles still exist.^{18,20,21} Therefore, how to further improve the tumor-targeting effect of these nanoparticles and achieve effective intracellular anticancer drug release has become a series of crucial issues at present.

In general, nano-sized nanoparticles exhibit passive tumor-targeting effects through the EPR effect.^{22,23} However, the EPR effect only leads to the accumulation of nanoparticles in tumor tissues, and the subsequent endocytosis of nanoparticles is usually hindered due to the weak specific interaction with tumor cell membranes.^{20–23} To address this issue, nanoparticles can be further modified with functional ligands to obtain active tumor-targeting effects. Folic acid (FA), which is considered to be a derivative of vitamin B, has a high affinity for the folate receptor (FR), which is overexpressed in most types of tumor cells, including lung cancer.^{24–26} Therefore, modification of folic acid has been widely used in active tumor-targeted drug delivery systems because it enhances accumulation at the intended tumor site, promotes intracellular internalization through folate receptor-mediated endocytosis, and thus increases the intracellular therapeutic concentration of anticancer drugs.^{24–28}

In this study, we developed FA-DTX-APs modified albumin polyester nanocarriers encapsulating docetaxel (DTX)-using PEG and PLGA as matrix materials and bovine serum albumin (BSA) as a backbone. These nanocarriers were further functionalized with FR-targeting FA. Featuring optimal physicochemical and biological properties, FA-DTX-APs enable localized, sustained, and controlled DTX release, effectively targeting and eradicating tumors. This innovative nanoformulation holds great potential in lung cancer treatment and clinical translation.

Materials and Methods

A549, NCI-H1650, BEAS-2B, and HUVEC cells were sourced from Beijing Beina Chuanglian Biotechnology Institute. Cell culture essentials including 1640 and DMEM media, PBS, FBS, and trypsin were obtained from Gibco. Chemicals such as propionate, mPEG₂₀₀₀-OH, stannous octanoate, ethionate, solvents (DCM, ethanol, chloroform), and BSA were purchased from Sigma, Beijing Chemical Industry Group, and Tianjin Hynes Biochemical Technology, respectively.

DTX (Purity: 99.94%) was acquired from Chongqing Taimeng Pharmaceutical, while MTT kit and biochemical reagents (NHS, EDC, FA, DAPI, FITC) were sourced from Beijing Chemical Factory, Murray (Shanghai) Biotechnology, Abcam, and Aladdin. Apoptosis detection (Alexa Fluor 488) and biomarker assay (AST, ALT, BUN, Cr, CK, LDH, FA ELISA) kits were procured from Invitrogen and R&D Systems (USA).

Preparation Process of Nanocarriers

A vacuum reaction flask was charged with 2 g of mPEG₂₀₀₀-OH and subsequently dehydrated under vacuum at 120°C. Then, 0.8 mg stannous octanoate, 0.32 g propanocarbonate, and 0.08 g ethanocarbonate were added. The reaction was heated to 150°C under 70 Pa vacuum and magnetically stirred (500 r/min) for 24 hours (h). The product was dissolved in dichloromethane, precipitated with ethanol, and dried under vacuum at 40°C to yield PEG-PLGA block copolymer. In a 250 mL round-bottom flask, 2 g of BSA was dissolved in 2 mL ultrapure water. While stirring at 500 r/min (24°C), ethanol was added slowly (0.5 mL/min) until complete. After 1 hour of stirring, 5 mL of a 1 g/mL PEG-PLGA chloroform solution was added, and the mixture was stirred overnight (500 r/min, 24°C). The organic solvent was removed by rotary evaporation, forming a polymer film. Further vacuum drying for 12 h removed residual solvent, and 50 mL PBS was added, followed by sonication (Power 27%, temperature 25°C, ultrasound 2 seconds, interval 1 second) for 30 minutes and stirring (500 r/min) for 12 h to produce modified albumin polyester nanocarriers (APs). To 1 mL of APs (200 mg/mL), 20 mg of DTX (0.1% Tween 80) was added and stirred (500 r/min) for 24 h. Dialysis (regenerated cellulose, pore size 22 mm, MWCO 10KD) for 12 h yielded DTX-encapsulated APs (DTX-APs). To 1 mL of DTX-APs, 10 mg each of EDC and NHS coupling agents, along with 60 µg of FA, were added and stirred (500 r/min) homogeneously at 4°C for 24 h to obtain FA-labeled DTX-APs (FA-DTX-APs) (Figure 1A). FA-DTX-APs were placed at 4°C for storage.

Physicochemical Characterization and Morphological Observation of Nanocarriers

10 µL of the sample was diluted in 2 mL of ultrapure water, and the particle size and potential of the nanocarriers were tested using a Malvern Nanoparticle Size and Zeta Potential Analyzer (Zetasizer Nano ZS) to test the change in the particle size of the FA-DTX-APs over 24 h to examine their suspension properties in solution. Fourier transform infrared spectroscopy (FTIR) was used to detect the FTIR spectra of the nanocarriers in the near-infrared region. The morphological features of the nanocarriers were observed using transmission electron microscopy (TEM).

Drug Release Performance Testing

The best absorption peak of DTX was determined by full wavelength scanning of DTX standard solution by ultraviolet spectrophotometer (UV) spectrophotometer. Subsequently, we configured DTX standard solutions with concentrations of 2, 5, 10, 20 and 50 µg/mL, tested the OD values using UV at a wavelength of 229 nm and plotted the standard curves corresponding to the concentration and absorbance of DTX. The encapsulation efficiency, drug loading efficiency and drug release profile of the drug were tested based on the standard curve of DTX. Encapsulation efficiency = (total amount of DTX - amount of free DTX) / total amount of DTX × 100%. Drug loading efficiency = (total amount of DTX - amount of DTX) / total amount of nanodrugs × 100%. FA-DTX-APs were centrifuged three times using ultrafiltration centrifuge tubes of Amicon Ultra-4 with a molecular weight of 20 kDa to remove unencapsulated free drug. FA-DTX-APs and DTX were dissolved in 0.1% Tween 80 PBS (pH = 7.4 and pH = 5.3) containing 0.1% Tween 80 PBS and placed in a constant temperature shaker at 37°C. A set volume of samples was periodically removed and subjected to UV absorbance assay, after which the tubes were supplemented with the same volume of PBS. The OD values were tested using UV at a wavelength of 229 nm, the free drug content was calculated and the drug release profile of the nanodrugs was plotted.

Cytotoxicity Testing of Nanocarriers

HUVEC and BEAS-2B cells were cultured at 37°C in a 5% CO₂ incubator. HUVEC and BEAS-2B cells were counted and added to 96-well plates (5×10³) and cultured for 24 h with a follow up medium change. Subsequently, different concentrations of nanocarrier drugs (10, 50, 100, 200, and 500 µg/mL) were added, and the incubation was continued for 48 h. 20 µL MTT (5 mg/mL) (C0009S) was added to each well, and incubation was continued for 4 h. The medium was

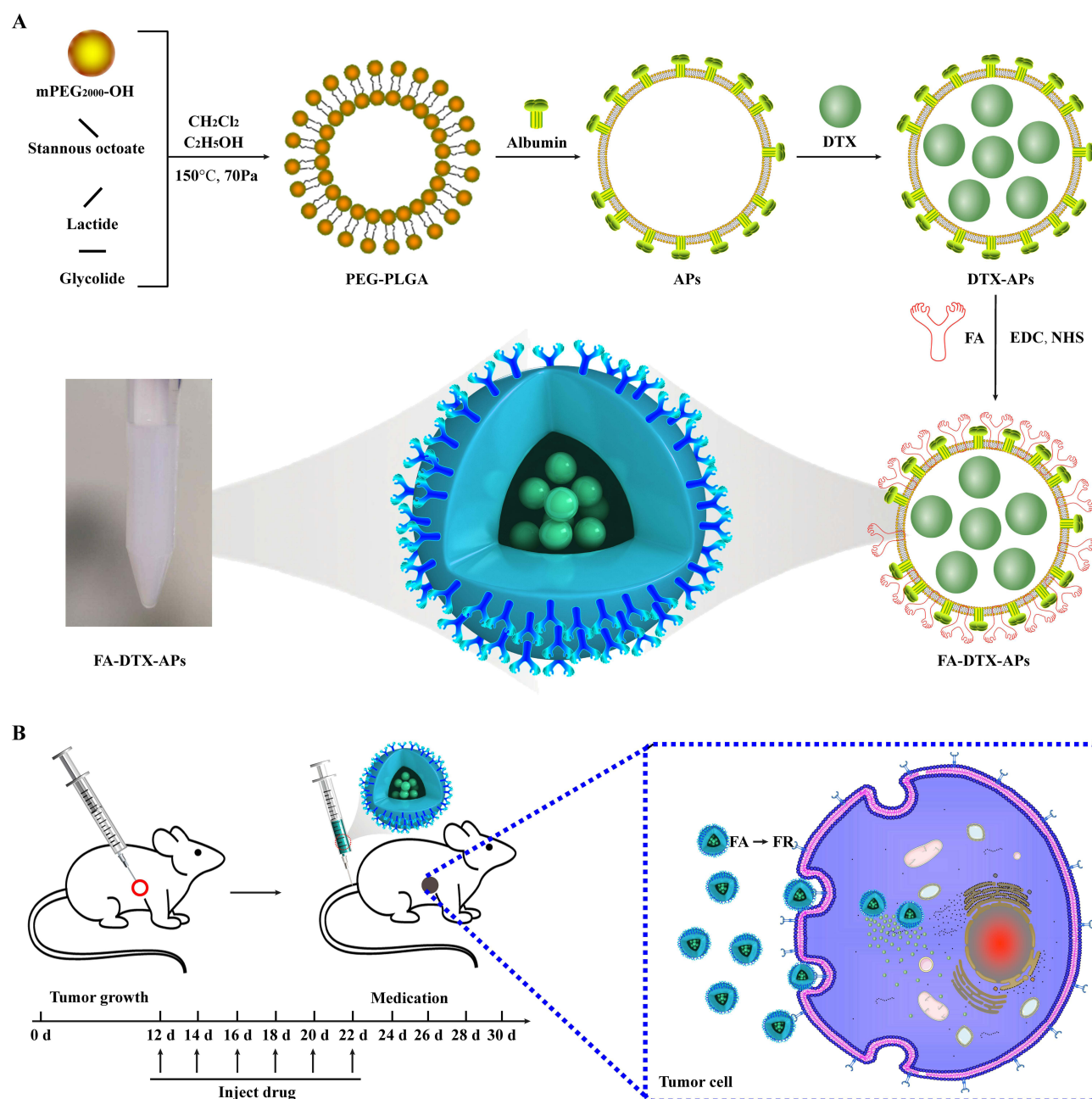


Figure 1 FA-DTX-APs preparation flow chart and animal experiment diagram. **(A)** Flow chart of the preparation of FA-DTX-APs; **(B)** Flow chart of animal experiments and the action of FA-DTX-APs in animals.

Abbreviations: DTX, docetaxel; PEG, polyethylene glycol; PLGA, poly(L-lactide-co-glycolide); FA, folic acid; FR, folate receptor; APs, albumin polyester nanocarriers; DTX-APs, DTX-encapsulated APs; FA-DTX-APs, FA-labeled DTX-APs; NHS, N-hydroxysuccinimide; EDC, 1-(3-Dimethylaminopropyl)-3-ethylcarbodiimide.

aspirated and the precipitate was left behind. After adding 150 μL DMSO to each well, it was placed on a shaker and shaken uniformly for 10 min. The absorbance value of each well was detected at 490 nm using a microplate reader (BIO-RAD 680) to calculate the cell viability. Cell viability (%) = (OD value of treatment group - OD value of blank group) / (OD value of control group - OD value of blank group) \times 100. The experiment was repeated three times for each group.

Effect of Nanomedicines on the Value-Added of Lung Cancer Cells

A549 and NCI-H1650 were counted and added to 96-well plates (5×10^3) and incubated for 24 h (37°C , 5% CO_2) and then the medium was changed. After adding the nanocarrier drug and incubating for different times (3, 6, 12, 24 and

48 h). 20 μ L MTT (5 mg/mL) was added to each well, and incubation was continued for 4 h. The medium was aspirated and the precipitate was left behind. After adding 150 μ L DMSO to each well, it was placed on a shaker and shaken uniformly for 10 min. The absorbance value of each well was detected at 490 nm using a microplate reader (BIO-RAD 680) to calculate the cell viability. Cytostatic rate (%) = $(1 - (\text{OD value of treatment group} - \text{OD value of blank group})) / (\text{OD value of control group} - \text{OD value of blank group}) \times 100$. The experiment was repeated three times for each group.

Effect of Nanomedicines on Apoptosis of Lung Cancer Cells

A549 and NCI-H1650 were counted and added to 6-well plates (5×10^5) and incubated for 24 h before changing the medium. Nanocarrier drugs were added and co-incubated for 48 h, and the cells were collected by centrifugation at 1200 rpm for 4 min. Add 10 μ L of propidium iodide reservoir solution (40301-B) and 10 μ L of RNase A (40301-A) solution to 0.5 mL of staining buffer (40301-C) and mix well for use. For each cell sample, 0.5 mL of configured propidium iodide staining solution was added, and the cells were gently mixed and resuspended. Incubate for 30 min at 37°C away from light and analyze the assay using a flow cytometer (NovoCyte).

Uptake of Nanomedicines by Lung Cancer Cell

A549 and NCI-H1650 cells in logarithmic growth phase were inoculated in 12-well plates with coverslips at a cell density of 2×10^5 /well and incubator at 37°C overnight. DTX was mixed with FITC at a certain molar ratio (1: 2) using DMSO as solvent. The reaction was carried out at 4°C under light protection with continuous stirring for 12 h. The unreacted FITC was removed after dialysis to obtain FITC-labeled DTX solution. The nanomedicine was mixed with DiIC16 at a certain molar ratio (1: 2) using DMSO as solvent. The reaction was carried out at 4°C under light protection with continuous stirring for 12 h. The unreacted FITC was removed after dialysis to obtain DiI-labeled nanodrug solution. The fluorescently labeled groups of drugs were added to the cells and cultured for 12 h. After adding DAPI staining for 10 min, the uptake of nanocarriers in the cells was observed using fluorescence microscopy.

Hemolytic Profile Testing of Nanomedicines

Mouse blood was collected by orbital blood sampling. Mouse blood was centrifuged at 2000 rpm for 10 min at 4°C, plasma was removed, and erythrocytes were resuspended with ice PBS. 200 μ L of nanocarrier drug at concentrations of 10–500 μ g/mL were added separately and incubated for 4 h at 37°C in a thermostat. The OD of the samples at 570 nm was measured by UV. Saline was used as the negative control and ultrapure water was used as the positive control. Hemolysis rate (%) = $(\text{OD value of the sample to be tested} - \text{OD value of the negative control tube}) / (\text{OD value of the positive control tube} - \text{OD value of the negative control}) \times 100$.²⁹

Antitumor Activity and Safety Evaluation of Nanomedicines in Mice

The animal study protocol was approved by the Experimental Animal Ethics Committee of Shanghai University (approval No. EAECSHU2023-0188) and performed following the Guide for the Use and Care of Laboratory Animals. Twenty-four BALB/c female nude mice were purchased from Shanghai Slaughter Laboratory Animal Co. After one week of acclimatization, the mice were tumor-bearing by subcutaneous injection of 0.1 mL (1×10^7 cells/mL) of A549 cells for 12 days and were randomly divided into the control group (NC), DTX-treated group, DTX-APs-treated group, and FA-DTX-APs-treated group, with 6 mice in each group. Drug treatment was administered by tail vein injection every other day from day 12 onwards, and the drug was continuously administered six times at a dose of 4 mg/kg (Figure 1B). After the injection of drug treatment, the tumor volume was weighed and measured every other day to calculate the tumor suppression rate, and the positivity of FA-positive cells in the tumor tissue was detected by FA ELISA antibody kit. Tumor inhibition rate = $1 - (\text{tumor mass/animal mass (experimental group)}) / (\text{tumor mass/animal mass (control group)})$. To further verify the in vivo biosafety of the drug, further serum biochemical indexes were examined at the end of the treatment, specifically: AST, ALT, BUN, Cr, CK, LDH, which were performed according to the instructions of the kit. The specific test method of the kit is as follows: Blood is centrifuged (3000 rpm) for 20 min and serum is collected. Prepare experimental standards, reagents and samples, add 50 μ L of samples to each well and incubate at 37°C for 30 min. Wash the plate 5 times and add 50 μ L of

enzyme reagent, incubate at 37°C for half an hour. After washing the plate 5 times, add 50 μL of color development solution A and B each, and incubate at 37°C for 15 min to develop the color. Finally, 50 μL of termination solution was added, followed by measuring the absorbance of each well at 450 nm. In addition, the livers, hearts, spleens, and kidneys of the mice in each group were removed and stained with hematoxylin-eosin (HE) to observe the changes.

Statistical Analysis

All data are expressed as mean (X) \pm standard deviation (S). All statistical data were repeated three times for the test. Significance of differences was tested using one-way ANOVA and paired t-tests. The analysis software was Graph Pad Prism 8.0.2, where * $P < 0.05$ means the difference is statistically significant; ** $P < 0.01$ means statistically significant.

Results

Physicochemical Characterization and Morphological Analysis of Nanocarriers

The particle size of FA-DTX-APs was 223.65 ± 6.83 nm, and the PDI was 0.172 ± 0.021 (Figure 2A). Zeta potential of FA-DTX-APs was 26.76 ± 3.15 mv (Figure 2B). The particle size increased with the increase of DTX drug content, and the particle size no longer increased when the mass ratio of DTX drug to APs was 1:10, and the PDIs were all less than 0.2 (Figure 2C and D). There was no significant increase in the potential with the increase of DTX drug content (Figure 2E). The particle size decreased slowly but without significant difference in the FA-DTX-APs solution during 24 h of standing, the particle sizes were all above 200 nm, and there was no significant change in the PDI, which indicated that the suspension properties of the FA-DTX-APs was good (Figure 2F and G). The results of the FTIR test showed that the particle sizes of the DTX drug and the APs were higher than 200 nm at $1450\text{--}1470\text{ cm}^{-1}$ and $1630\text{--}1760\text{ cm}^{-1}$, which correspond to the absorption bands of methyl group and those belonging to the carbonyl group due to the carbonyl stretching, were found as typical absorption peaks. Between the absorption bands at $2850\text{--}2920\text{ cm}^{-1}$, a smaller absorption peak appeared for APs and DTX, and two absorption peaks appeared for both FA-DTX-APs and DTX-APs with a significant enhancement of the absorption peaks, suggesting that DTX had been successfully encapsulated into the APs (Figure 2H). TEM observed that FA-DTX-APs were well dispersed without agglomeration and characterized by vesicles (Figure 2I).

Encapsulation Efficiency and in vitro Drug Release of Nanomedicines

The UV scanning curve showed the best UV absorption peak of DTX at 229 nm (Figure 3A). The linear regression of DTX concentration on absorbance showed a good linear relationship with the regression equation: $y = 0.0296x + 0.1409$, $R^2 = 0.9998$ (Figure 3B). The results of the encapsulation efficiency test showed that when the ratio of DTX: APs was less than 1:10, the encapsulation efficiency did not change significantly, but with the increase of DTX, the encapsulation efficiency of DTX was gradually decreasing (Figure 3C). The results of the drug loading efficiency test showed that when the ratio of DTX: APs was less than 1:10, the drug loading efficiency gradually increased, but with the increase of the proportion of DTX, the drug loading efficiency of DTX was gradually stabilized (Figure 3D). Therefore, 1:10 was the optimal mass ratio of DTX to APs, in which both encapsulation efficiency and drug loading efficiency could be optimized, with an encapsulation efficiency of $(96.19 \pm 3.27)\%$ and a drug loading efficiency of $(9.75 \pm 0.38)\%$ (Figure 3C and D). In a neutral environment with pH 7.4, the cumulative release rate of DTX reached more than 80% at 2 h, whereas the cumulative release rate of FA-DTX-APs was $(61.6 \pm 3.58)\%$ at 24 h (Figure 3E), indicating that the FA-DTX-APs possessed a significant drug slow release property. In an acidic environment with pH 5.4, the cumulative release rate of DTX reached more than 80% at 4 h, whereas the cumulative release rate of FA-DTX-APs was $(73.6 \pm 3.65)\%$ at 24 h (Figure 3F). This indicated that FA-DTX-APs not only possessed obvious drug slow-release properties, but also had the pH-responsive characteristics, which were capable of accelerating the release of the drug in an acidic environment.

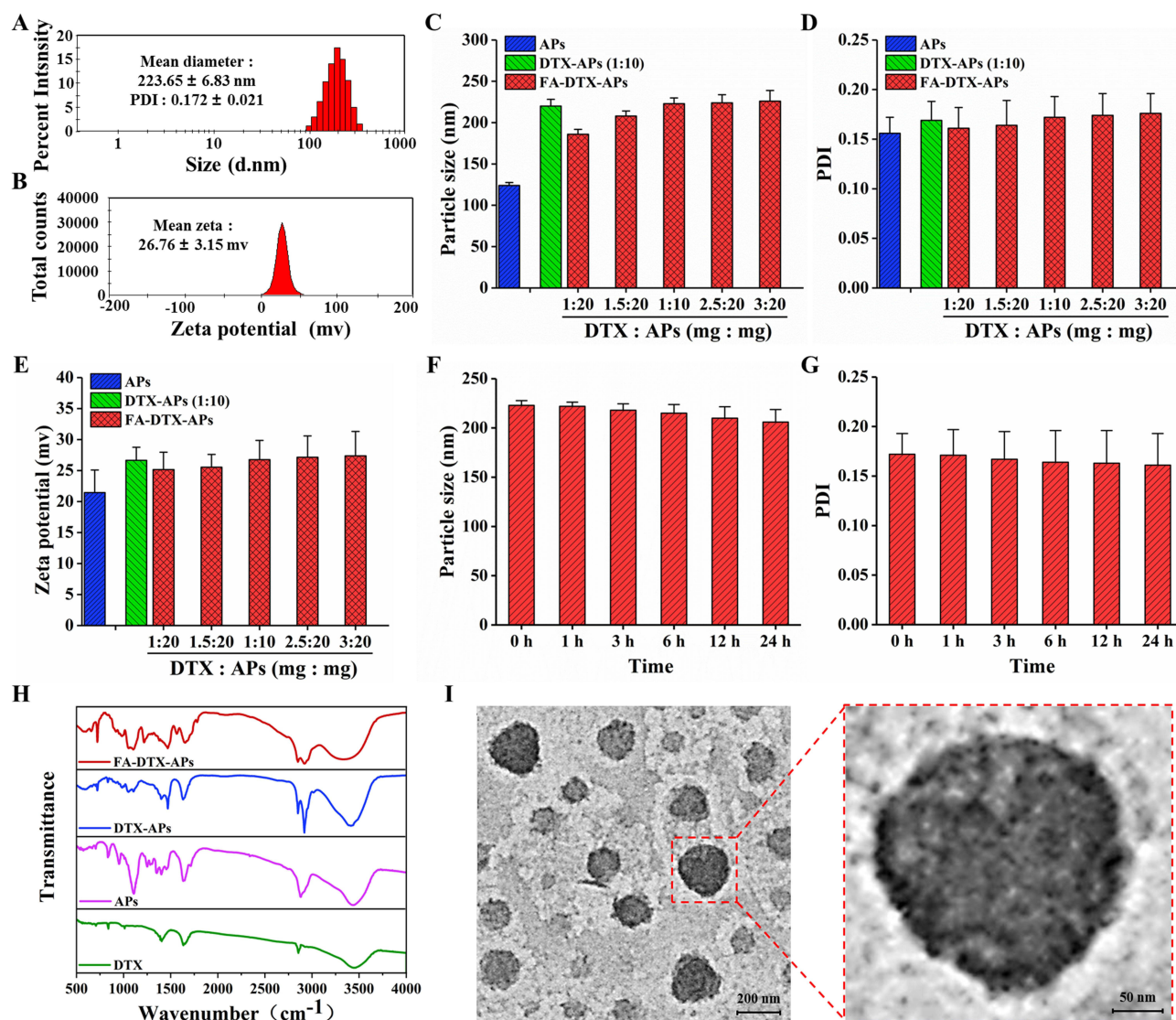


Figure 2 Physicochemical characterization tests of nanocarriers. (A) Particle size distribution of FA-DTX-APs; (B) Potential distribution of FA-DTX-APs; (C) Particle size test of different nanocarriers; (D) PDI of different nanocarriers; (E) Potential test of different nanocarriers; (F) Particle size test of FA-DTX-APs after different time of resting; (G) PDI of FA-DTX-APs after different time of resting; (H) Nanocarriers FTIR test; (I) TEM test of FA-DTX-APs. All experiments were repeated three times.

Analysis of Biological Properties of Nanomedicines

There was no significant difference in the toxicity of nanocarriers to HUVEC and BEAS-2B cells within the range of safe use concentration ($\leq 100 \mu\text{g/mL}$), with cell survival above 90%, and the cytotoxicity of APs, DTX-APs, and FA-DTX-APs was significantly increased when the nanocarriers were used at a concentration $\geq 200 \mu\text{g/mL}$ (Figure 4A and B). Compared with the DTX group, APs had no inhibitory effect on A549 and NCI-H1650 cells, and DTX-APs and FA-DTX-APs had obvious value-added inhibitory effects on A549 and NCI-H1650 cells, and the value-added inhibitory effects on lung cancer cells were more pronounced due to the ability of FA-DTX-APs to recognize lung cancer cells by targeting (Figure 4C and D). The results of apoptosis experiments showed (Figure 4E and F) that APs did not affect the apoptosis rate of A549 and NCI-H1650 cells, and their late apoptosis rates on cells were all within 5%. Compared with DTX and DTX-APs, FA-DTX-APs could significantly promote apoptosis in A549 and NCI-H1650 cells.

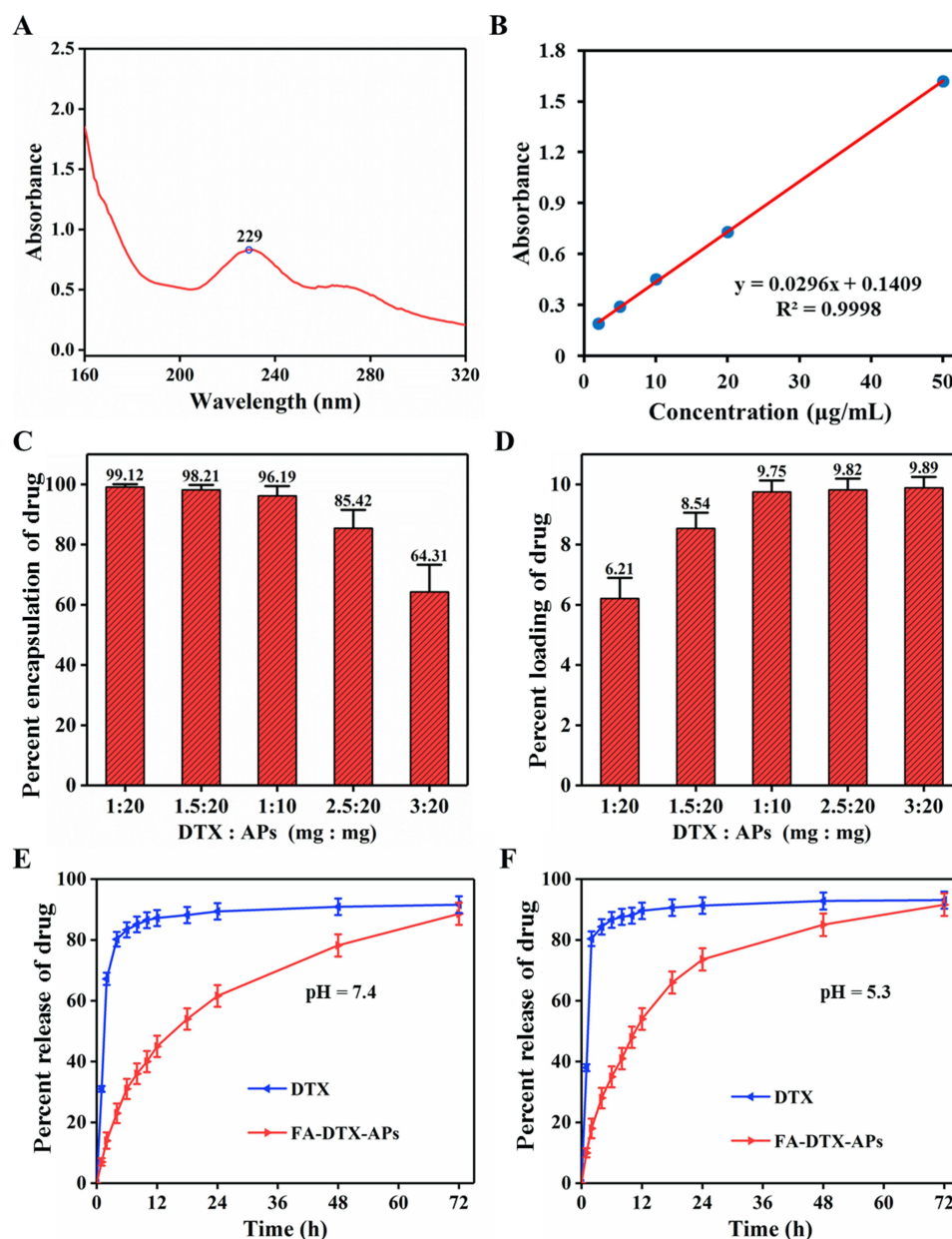


Figure 3 Encapsulation efficiency test and in vitro drug release test. (A) UV scanning curves of DTX; (B) Standard curves of DTX; (C) Encapsulation efficiency test after addition of different levels of DTX drug to FA-DTX-APs; (D) Drug loading efficiency test after addition of different levels of DTX drug to FA-DTX-APs; (E) Drug release profiles of DTX and FA-DTX-APs at pH = 7.4 (37°C); (F) Drug release profiles of DTX and FA-DTX-APs at pH = 5.3 (37°C). All experiments were repeated three times.

Analysis of Lung Cancer Cell Uptake of Nanomedicines and Hemolysis of Nanomedicines

Lung cancer intracellular uptake experiments showed (Figure 5A and B) that FA-DTX-APs could be effectively taken up by lung cancer cells due to its ability to target recognition of lung cancer cells, thus efficiently entering into A549 and NCI-H1650 cells. The results of hemolysis experiments showed that when the erythrocyte suspension was added to water, red hemolysis was seen in the supernatant after centrifugation, indicating that hemolysis reaction occurred; on the contrary, adding different concentrations of FA-DTX-APs solutions of 10–500 μg/mL to the erythrocyte suspension did not cause obvious hemolysis, and the supernatants were all transparent (Figure 5C). Measuring the absorbance of the supernatants with an enzyme marker, it can be found that the supernatants did not change significantly after the addition of FA-DTX-APs, and none of the hemolysis rates exceeded 5%, indicating that the erythrocytes were not ruptured (Figure 5D). This also confirms that FA-DTX-APs can well maintain the intact structure of erythrocyte membrane when it interacts with the erythrocyte membrane and has good biocompatibility.

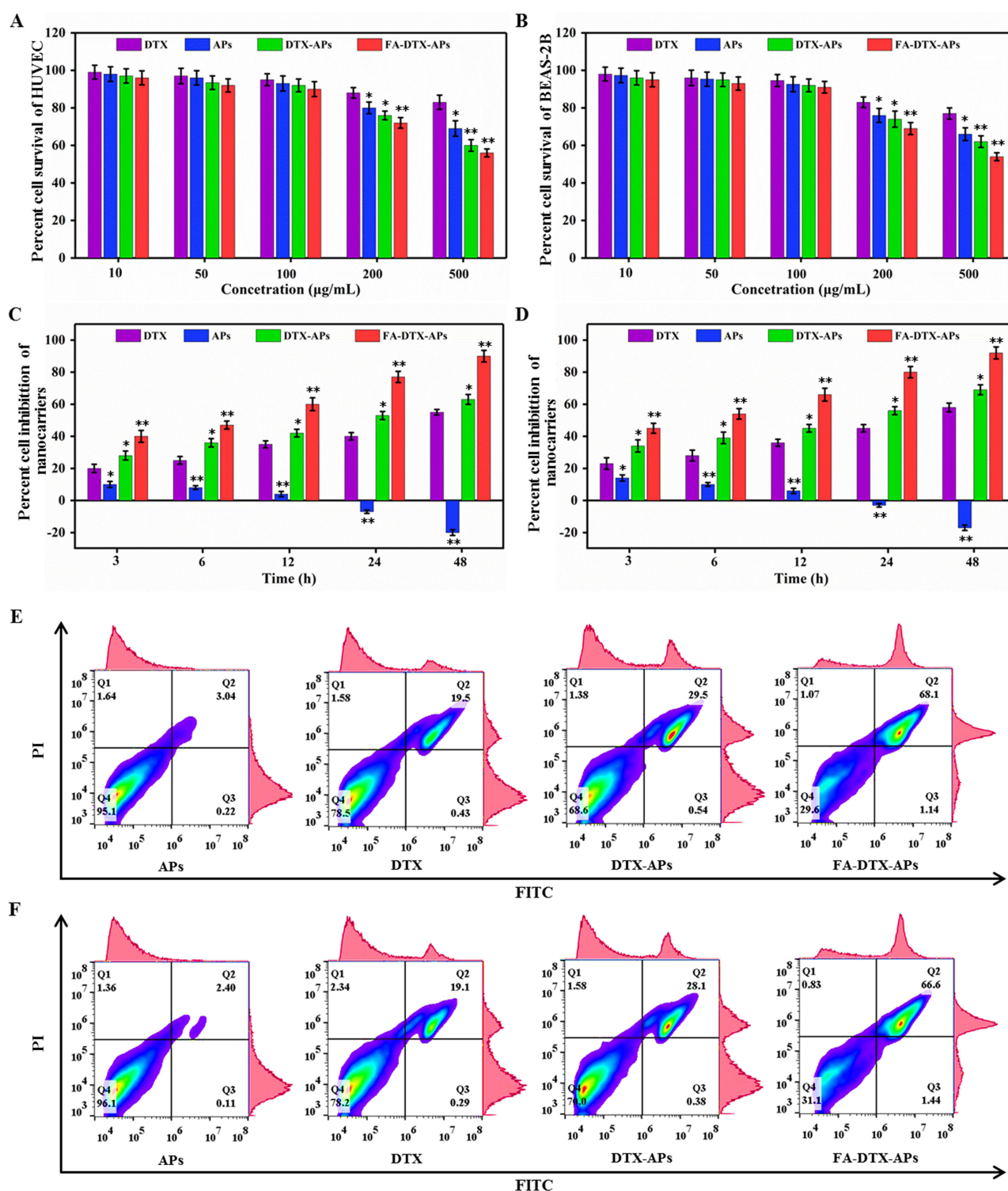


Figure 4 The effects of nanocarriers on cell toxicity, proliferation and apoptosis were examined by cellular assays. **(A)** Toxicity of nanocarriers on HUVEC cells; **(B)** Toxicity of nanocarriers on BEAS-2B cells; **(C)** Proliferative effects of nanocarriers on A549 cells; **(D)** Proliferative effects of nanocarriers on NCI-H1650 cells; **(E)** Apoptotic effects of nanocarriers on A549 cells; **(F)** Apoptotic effects of nanocarriers on NCI-H1650 cells. * $P < 0.05$, ** $P < 0.01$. All experiments were repeated three times.

Evaluation of Anti-Tumor Activity of Nanomedicines in Mice

The weight change curve of the mice showed (Figure 6A) that the mice in the free DTX group, after administration of the drug, showed a significant decrease in body weight, and by the end of the treatment, the average weight of the DTX mice

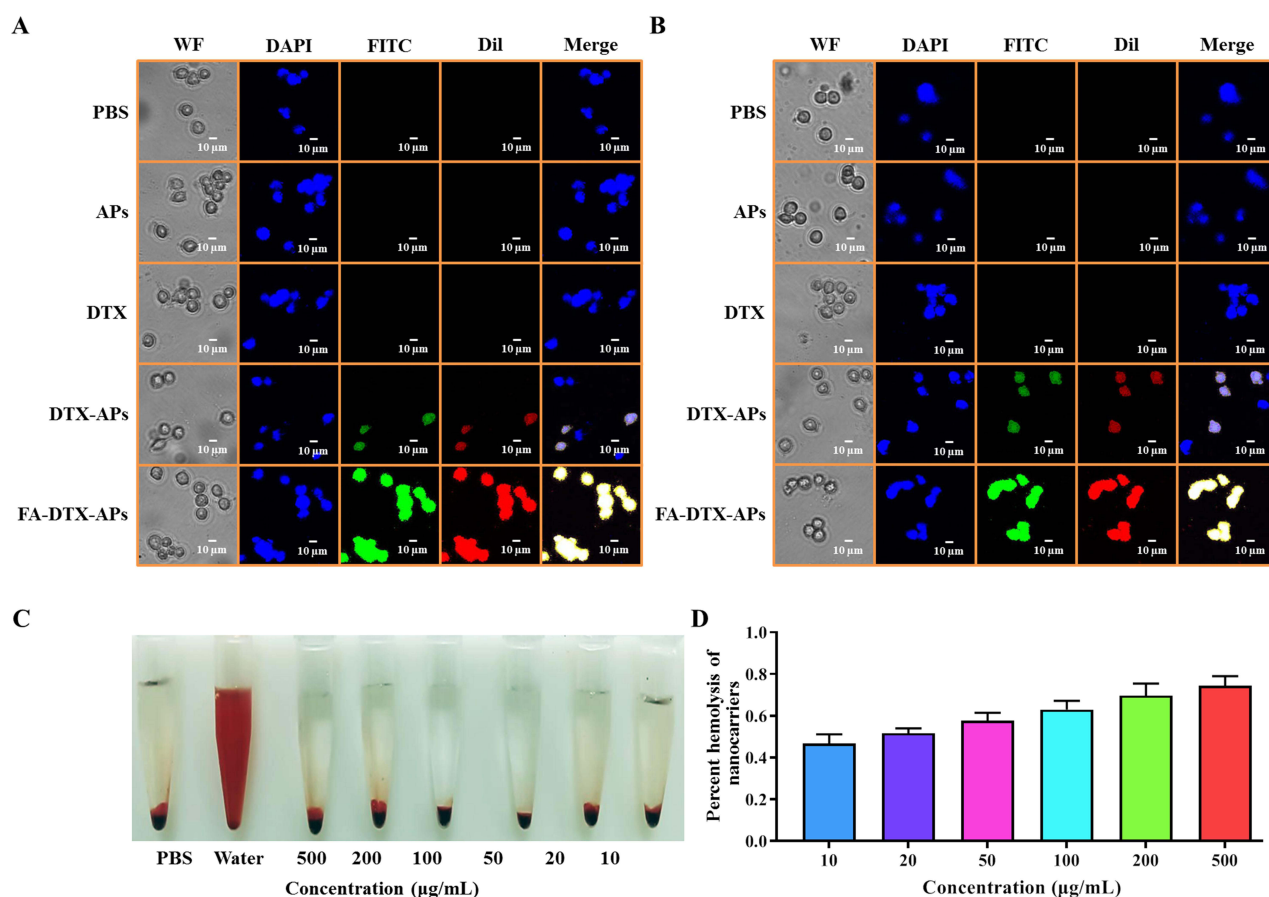


Figure 5 Lung cancer intracellular uptake effect and hemolysis test of nanocarriers. (A) Uptake of nanocarriers by A549 cells; (B) Uptake of nanocarriers by NCI-H1650 cells; (C) Hemolysis experiments with different concentrations of nanocarriers (37°C); (D) Hemolysis rate statistics with different concentrations of nanocarriers (37°C).

was about (17.62 ± 0.68) g, which was statistically different from the post-treatment body weight of the DTX-APs and the FA-DTX-APs ($P < 0.05$). The weight loss was considered to be due to the digestive system toxicity of DTX. There was no significant change in body weight before and after treatment with DTX-APs and FA-DTX-APs, which further verified that the nanocarriers were more protective against the drug and the nanocarrier drug had less nonspecific distribution and fewer toxicities compared with conventional DTX. The statistical results of tumor volume changes and tumor inhibition rate showed (Figure 6B-D) that DTX, DTX-APs and FA-DTX-APs all had obvious anti-tumor effects after treatment, but FA-DTX-APs had the best anti-tumor effect and the rate of FA-positive cells in tumor tissues was obviously the least after treatment. It indicated that the nanocarriers were able to recognize FA-positive lung cancer tumor cells after being modified by FA, which further enhanced the anti-tumor effect of FA-DTX-APs.

Safety Evaluation of Nanomedicines in Mice

The assessment of liver function impairment showed (Figure 7A and B) that ALT and AST were mildly increased to varying degrees in all groups after drug treatment, more significantly in DTX, but there was no statistically significant difference between the groups. The assessment of renal impairment showed (Figure 7C and D) that BUN was mildly increased in all groups after drug treatment, with DTX being more significant, but there was no statistically significant difference between the groups, and there was no significant effect of drugs on creatinine in all groups. Assessment of cardiac impairment showed (Figure 7E and F) that CK and LDH were mildly increased in all groups after drug treatment, more significantly in DTX. At the end of the treatment, HE staining was taken from the heart, liver, spleen and kidney of the mice, and no obvious macromolecular deposition was seen, and no obvious tissue structure destruction disorder was

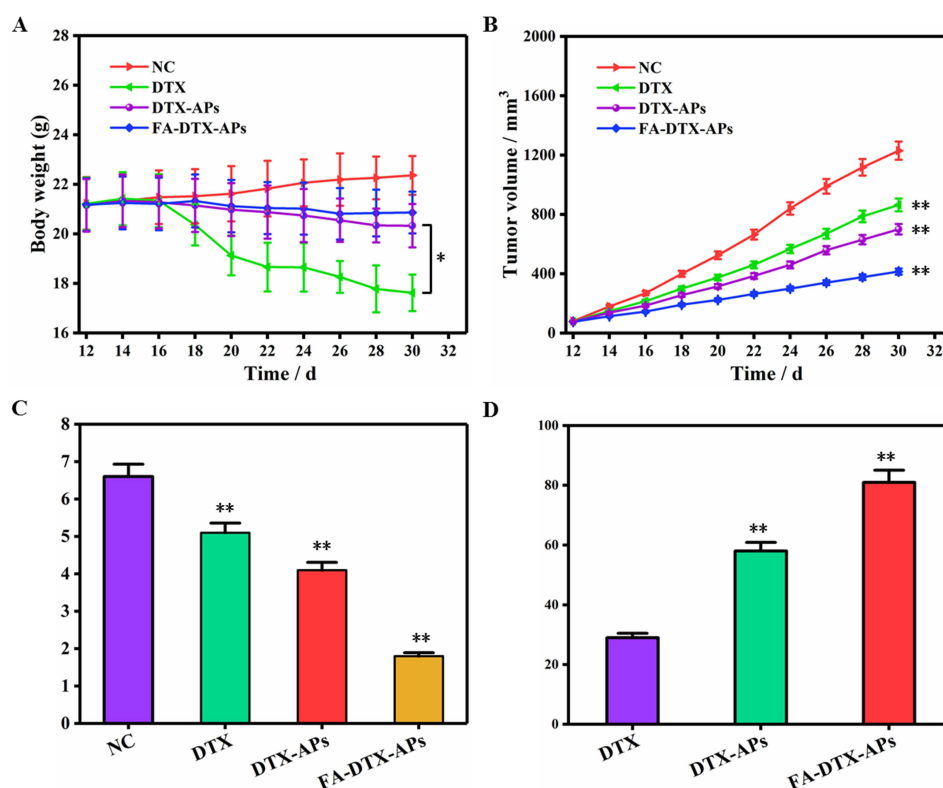


Figure 6 Study on antitumor activity of nanocarriers in vivo. **(A)** Changes in body weight of mice during treatment with nanocarrier drug; **(B)** Changes in tumor volume during treatment with nanocarrier drug; **(C)** Changes in the rate of FA-positive cells in tumor tissues at the end of treatment; **(D)** Tumor inhibition rate at the end of treatment. ** $P < 0.01$. All experiments were repeated three times.

observed, which was not significantly different from that of the control group (Figure 7G). It was further verified that DTX after encapsulation by nanocarriers had relatively little effect on the organs and was biosafe.

Discussion

Lung cancer stands as one of the most prevalent cancers, with non-small cell lung cancer accounting for approximately 80% of all lung cancer cases.³⁰ While the non-selective distribution of these drugs within the body, inadvertently damages normal tissues, leading to toxic side effects across various physiological systems.^{31–33} These adverse effects significantly constrain the clinical application of chemotherapeutic drugs. Moreover, despite their potent anti-tumor activity, certain chemotherapeutic agents are hindered by their hydrophobicity or short metabolic half-life, necessitating enhancements in their pharmacokinetics to optimize therapeutic outcomes.^{34,35} By encapsulating drugs within nanocarriers for in vivo delivery, this innovative approach augments drug stability, enhances tissue penetration, and precisely regulates drug distribution and release kinetics within the body. Consequently, it significantly improves drug bioavailability, paving the way for more effective and safer lung cancer treatments.^{36,37}

Currently, FDA has granted approval for over 900 nano-anti-tumor drugs to proceed into clinical trials, yet only a handful have successfully transitioned to the market for clinical use.³⁸ While some of these drugs' side effects can be mitigated, they remain unavoidable, and the nano-anti-tumor drugs under development have yet to fulfill our aspirations for safe, efficient, and low-toxicity therapeutic outcomes.^{39,40} PLGA, a biodegradable functional polymer organic complex, boasts improved compatibility, non-toxicity, excellent encapsulation capabilities, and film-forming properties.^{15–17} Albumin, on the other hand, exhibits a remarkable ability to bind with a wide array of drugs and bioactive agents, including chemotherapeutic drugs and antibiotics, in vivo, and possesses a prolonged half-life and robust stability.^{18,19} Furthermore, PEG, a commonly employed polymer carrier, can modify nanocarriers like liposomes, albumin, and PLGA, enhancing their water solubility.⁴¹

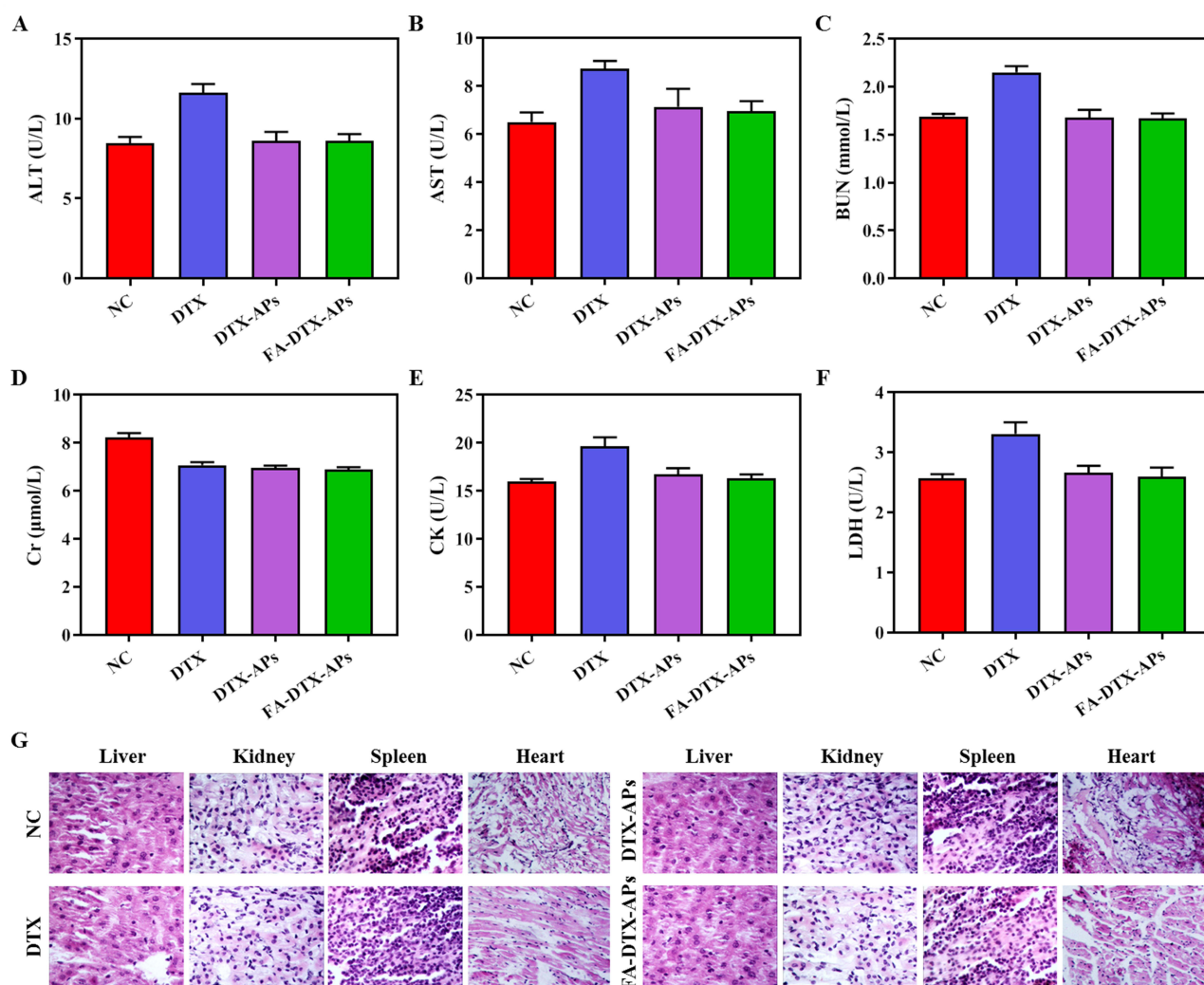


Figure 7 Study on serological biochemical toxicity and organ toxicity damage after drug treatment. (A). Detection of ALT content in blood of mice; (B) Detection of AST content in blood of mice; (C) Detection of BUN content in blood of mice; (D) Detection of Cr content in blood of mice; (E) Detection of CK content in blood of mice; (F) Detection of LDH content in blood of mice; (G) HE staining of various organs of mice. All experiments were repeated three times.

Unlike our previous focus on studying PEG-functionalized liposomes as a novel drug delivery system to meet the requirements of respiratory administration,⁴² in this study, we have developed a novel folate-targeted modified albumin polyester nanocarrier, FA-DTX-APs, which utilizes folate as the targeting molecule to achieve precise targeted delivery to lung cancer cells, thereby enhancing the targeting efficiency and therapeutic effects of chemotherapy drugs, including Docetaxel (DTX). FA-DTX-APs exhibit long-lasting slow-release characteristics, especially accelerated release in acidic environments, which helps to more effectively release drugs in the tumor microenvironment while reducing nonspecific distribution of drugs in normal tissues and reducing side effects. Experimental results show that FA-DTX-APs can efficiently recognize and enter lung cancer cells, significantly inhibit the growth of lung cancer cells, and demonstrate superior anti-tumor effects compared to traditional drug delivery methods. This innovative approach aims to address the limitations of current nanomedicines and pave the way for more effective and safer anti-tumor treatments.

Nanomedicine delivery systems have been widely studied in oncology therapy for their ability to improve the pharmacokinetic behavior of drugs, target delivery of active drug ingredients to the lesion, and control drug release. Alassaif et al⁴³ synthesized nanodrugs using chitosan and PLGA composite microspheres as a carrier for carboplatin, which were uniformly spherical in shape, with a particle size of about 156 nm, had a high encapsulation efficiency and could maintain stability for a long period of time, and had a higher therapeutic efficacy against PEO1 cells. Włodarczyk

et al⁴⁴ prepared a PLGA nanomedicine encapsulated with carboplatin, which was spherical in shape, uniform in size, with an average particle size of 110 nm, remained stable in serum, and showed pH-dependent PEG breakage and drug release properties, which resulted in greater efficacy against ovarian cancer cells. Zhu et al⁴⁵ prepared PLGA nanodrugs encapsulated with dual drugs, which were uniform in size, regular in morphology, spherical in shape and had an average particle size of 637.4 nm, which could specifically target ovarian cancer cells and significantly inhibit the growth of transplanted tumors. Paswan et al⁴⁶ used hyaluronic acid as a ligand to actively target CD44 receptors on the surface of breast cancer cells and synthesized PLGA-PEG coupling, which had a spherical shape, smooth surface, and a particle size of 294.8 nm, and possessed the characteristics of active targeting and delivery, which could improve the anti-breast cancer effect of the drug and reduce the toxic and side effects. Iqbal et al⁴⁷ used albumin as a tumor homing agent targeting breast cancer to prepare nanomedicine, which was spherical in shape with an average particle size of 120.5 nm, with a narrow particle size distribution, high drug loading capacity, high encapsulation efficiency, pH-responsive controlled release and active targeted drug delivery, and was able to significantly inhibit the growth of tumor cells.

The results indicated that FA-DTX-APs exhibited superior physicochemical characteristics, including enhanced dispersibility, suspension properties, and a precise particle size of 223.65 ± 6.83 nm, facilitating efficient cellular uptake.⁴⁸ In addition, when the mass ratio of DTX to AP reached 1:10, the particle size of FA-DTX-APs no longer increased, which was because the encapsulation efficiency of DTX had reached saturation, and continued encapsulation of DTX might lead to the rupture or fusion of nanomedicines. Their positive charge facilitated electrostatic interactions with negatively charged cell membranes, boosting drug delivery efficiency.⁴⁹ Both FAM and TEM imaging confirmed the vesicular morphology and uniform dispersion of FA-DTX-APs, corroborating DLS measurements. As pH-responsive nanocarriers, FA-DTX-APs remained structurally stable in normal tissues but swiftly released the drug in the acidic tumor microenvironment due to weakened drug-carrier interactions.⁵⁰ This pH-sensitivity accelerated drug release, leveraging the lower pH of tumor tissues as a stimulus for controlled delivery. The use of FA-DTX-APs in the concentration range of 10–100 $\mu\text{g/mL}$ did not result in a statistically significant dose-dependent decrease in cell viability, and the cell survival rates were all higher than 90%. This indicates that PLGA-PEG nanoparticles have good biocompatibility and can be used as carriers in this concentration range. Typically, preparations with cell survival above 80% are considered safe. Therefore, we used 100 $\mu\text{g/mL}$ as the safe use concentration for subsequent experimental studies.⁵¹ Cellular value-added experiments showed that the cytotoxic effects of DTX dominated when DTX was encapsulated in APs. In addition, FA-DTX-APs active targeting of folate receptor (FR)-overexpressed lung cancer cells^{24–28} enhanced cellular uptake and markedly inhibited lung cancer cell proliferation while promoting apoptosis. FA-DTX-APs also showed excellent biocompatibility, with a hemolysis rate below 1%, adhering to the medical standard of $< 5\%$.⁵² Notably, the observed weight loss in mice treated with DTX alone was attributed to gastrointestinal toxicity, a common side effect of traditional chemotherapeutics.^{53,54} In contrast, FA-DTX-APs displayed superior antitumor efficacy with minimal organ damage, as evidenced by serum biochemical analyses, indicating improved biosafety over unconjugated DTX. Collectively, these findings underscore the immense potential of FA-DTX-APs as an effective and safe antitumor drug for lung cancer treatment, holding promising clinical translation prospects.

Although FA-DTX-APs have numerous advantages as drug carriers, there are still some urgent problems to be solved. On the one hand, there is still no complete biosafety evaluation system for FA-DTX-APs, especially the evaluation of *in vivo* biological effects is still in the primary stage, and more *in vivo* and *in vitro* evaluation experiments need to be added in the future and the experimental sample size needs to be increased for validation. On the other hand, we preliminarily confirmed that FA-DTX-APs have pH-responsive drug release kinetic properties, but more mechanistic support is needed, and more experiments and subgroups need to be designed in the future to jointly study the cumulative release of the drug *in vitro* with the antitumor activity *in vivo*. Finally, the specific process of absorption, distribution, and metabolism of FA-DTX-APs *in vivo* is still unclear, and more experiments such as pharmacokinetics and biodistribution need to be designed in the future, as well as comparative studies with other more advanced lung cancer nanodrugs. In conclusion, our results demonstrate the efficacy of albumin nanocarrier-based drug delivery systems for lung cancer treatment and are believed to be tested in preclinical and clinical settings in the near future to develop an alternative cost-effective lung cancer treatment.

Conclusions

In this investigation, we devised a folate acid (FA)-targeted modified albumin polyester nanocarrier encapsulating docetaxel (DTX). Boasting an impressive encapsulation efficiency, drug loading capacity, and excellent biocompatibility, the nanocarrier facilitates continuous, controlled release of DTX directly to tumor sites, ensuring safe and efficient eradication of cancer cells. This promising nanoformulation holds significant potential for lung cancer treatment, representing a crucial advancement in the quest for effective therapeutic strategies against this devastating disease.

Data Sharing Statement

Data will be made available on request.

Author Contributions

All authors made a significant contribution to the work reported, whether that is in the conception, study design, execution, acquisition of data, analysis and interpretation, or in all these areas; took part in drafting, revising or critically reviewing the article; gave final approval of the version to be published; have agreed on the journal to which the article has been submitted; and agree to be accountable for all aspects of the work.

Funding

The funding for this study comes from the Minhang District specialty (ZYPP04).

Disclosure

The authors declare no conflict of interest.

References

1. Li C, Lei S, Ding L, et al. Global burden and trends of lung cancer incidence and mortality. *Chin Med J*. 2023;136(13):1583–1590. doi:10.1097/CM9.00000000000002529
2. El-Hussein A, Manoto SL, Ombinda-Lemboumba S, Alrowaili ZA, Mthunzi-Kufa P. A review of chemotherapy and photodynamic therapy for lung cancer treatment. *Anticancer Agents Med Chem*. 2021;21(2):149–161. doi:10.2174/18715206MTA1uNjQp3
3. Livinghouse CL, Latifi K, Asous AG, et al. Dose-limiting pulmonary toxicity in a phase 1/2 study of radiation and chemotherapy with ipilimumab followed by nivolumab for patients with stage 3 unresectable non-small cell lung cancer. *Int J Radiat Oncol Biol Phys*. 2023;116(4):837–848. doi:10.1016/j.ijrobp.2023.01.006
4. Gray JE, Hsu H, Younan D, et al. Real-world outcomes in patients with KRAS G12C-mutated advanced non-small cell lung cancer treated with docetaxel in second-line or beyond. *Lung Cancer*. 2023;181:107260. doi:10.1016/j.lungcan.2023.107260
5. Landi L, Delmonte A, Bonetti A, et al. Combi-TED: a new trial testing Tedopi® with docetaxel or nivolumab in metastatic non-small-cell lung cancer progressing after first line. *Future Oncol*. 2022;18(40):4457–4464. doi:10.2217/fon-2022-0913
6. Su Z, Zhao J, Zhao X, Xie J, Li M, Zhao D. Preclinical evaluation of albumin-bound docetaxel nanoparticles as potential anti-cancer products. *Int J Pharm*. 2023;635:122711. doi:10.1016/j.ijpharm.2023.122711
7. Holsæter AM, Wizgird K, Karlsen I, Hemmingsen JF, Brandl M, Škalko-Basnet N. How docetaxel entrapment, vesicle size, zeta potential and stability change with liposome composition-A formulation screening study. *Eur J Pharm Sci*. 2022;177:106267. doi:10.1016/j.ejps.2022.106267
8. Han S, Sun R, Su H, et al. Delivery of docetaxel using pH-sensitive liposomes based on D- α -tocopheryl poly(2-ethyl-2-oxazoline) succinate: comparison with PEGylated liposomes. *Asian J Pharm Sci*. 2019;14(4):391–404. doi:10.1016/j.ajps.2018.07.005
9. Nezir AE, Bolat ZB, Ozturk N, et al. Targeting prostate cancer with docetaxel-loaded peptide 563-conjugated PEtOx-co-PEI30%-b-PCL polymeric micelle nanocarriers. *Amino Acids*. 2023;55(8):1023–1037. doi:10.1007/s00726-023-03292-3
10. Paliashvili K, Popov A, Kalber TL, et al. Peritumoral delivery of Docetaxel-TIPS microparticles for prostate cancer adjuvant therapy. *Adv Ther*. 2021;4(2):2000179. doi:10.1002/adtp.202000179
11. Entzian K, Aigner A. Drug delivery by ultrasound-responsive nanocarriers for cancer treatment. *Pharmaceutics*. 2021;13(8):1135. doi:10.3390/pharmaceutics13081135
12. Li C, Wang Z, Lei H, Zhang D. Recent progress in nanotechnology-based drug carriers for resveratrol delivery. *Drug Deliv*. 2023;30(1):2174206. doi:10.1080/10717544.2023.2174206
13. Bansal KK, Wilen CE, Rosenholm JM. Synthetic polymers in translational nanomedicine: from concept to prospective products. *Curr Pharm Des*. 2023;29(29):2277–2280. doi:10.2174/0113816128276471231010045123
14. Ramirez-Garcia PD, Veldhuis NA, Bunnett NW, Davis TP. Targeting endosomal receptors, a new direction for polymers in nanomedicine. *J Mater Chem B*. 2023;11(24):5390–5399. doi:10.1039/D3TB00156C
15. Dodda JM, Remiš T, Rotimi S, Yeh YC. Progress in the drug encapsulation of poly (lactic-co-glycolic acid) and folate-decorated poly (ethylene glycol)-poly (lactic-co-glycolic acid) conjugates for selective cancer treatment. *J Mater Chem B*. 2022;10(22):4127–4141. doi:10.1039/D2TB00469K

16. Lee CK, Atibalentja DF, Yao LE, Park J, Kuruvilla S, Felsher DW. Anti-PD-L1 F(ab) conjugated PEG-PLGA nanoparticle enhances immune checkpoint therapy. *Nanotheranostics*. 2022;6(3):243–255. doi:10.7150/ntno.65544
17. Zhang D, Liu L, Wang J, et al. Drug-loaded PEG-PLGA nanoparticles for cancer treatment. *Front Pharmacol*. 2022;13:990505. doi:10.3389/fphar.2022.990505
18. Ganguly SC, Mahanti B, Ganguly S, Majumdar S. Bovine serum albumin as a nanocarrier for efficient encapsulation of hydrophobic garcinol-A strategy for modifying the in vitro drug release kinetics. *Int J Biol Macromol*. 2024;278(Pt 1):134651. doi:10.1016/j.ijbiomac.2024.134651
19. Wang D, Chen W, Li H, et al. Folate-receptor mediated pH/reduction-responsive biomimetic nanoparticles for dually activated multi-stage anticancer drug delivery. *Int J Pharm*. 2020;585:119456. doi:10.1016/j.ijpharm.2020.119456
20. Wei G, Zhang S, Yu S, Lu W. Intravital microscopy reveals endothelial transcytosis contributing to significant tumor accumulation of albumin nanoparticles. *Pharmaceutics*. 2023;15(2):519. doi:10.3390/pharmaceutics15020519
21. Takakura Y, Takahashi Y. Strategies for persistent retention of macromolecules and nanoparticles in the blood circulation. *J Control Release*. 2022;350:486–493. doi:10.1016/j.jconrel.2022.05.063
22. Xu W, Yang S, Lu L, et al. Influence of lung cancer model characteristics on tumor targeting behavior of nanodrugs. *J Control Release*. 2023;354:538–553. doi:10.1016/j.jconrel.2023.01.026
23. Gawali P, Saraswat A, Bhide S, Gupta S, Patel K. Human solid tumors and clinical relevance of the enhanced permeation and retention effect: a 'golden gate' for nanomedicine in preclinical studies? *Nanomedicine*. 2023;18(2):169–190. doi:10.2217/nnm-2022-0257
24. Kesharwani P, Halwai K, Jha SK, et al. Folate-engineered chitosan nanoparticles: next-generation anticancer nanocarriers. *mol Cancer*. 2024;23(1):244. doi:10.1186/s12943-024-02163-z
25. Zhao Y, Jia C, Yao Z, et al. Dexamethasone pretreatment potentiates a folic acid-functionalized delivery system for enhanced lung cancer therapy. *Mol Pharm*. 2024;21(3):1077–1089. doi:10.1021/acs.molpharmaceut.3c00472
26. Azari F, Zhang K, Kennedy G, et al. Prospective validation of tumor folate receptor expression density with the association of pafolacianine fluorescence during intraoperative molecular imaging-guided lung cancer resections. *Eur J Nucl Med Mol Imaging*. 2023;50(8):2453–2465. doi:10.1007/s00259-023-06141-3
27. Pilch J, Kowalik P, Kowalczyk A, et al. Folate-targeting quantum dots- β -cyclodextrin nanocarrier for efficient delivery of unsymmetrical bisacridines to lung and prostate cancer cells. *Int J mol Sci*. 2022;23(3):1261. doi:10.3390/ijms23031261
28. Essa ML, Elashkar AA, Hanafy NAN, Saied EM, El-Kemary M. Dual targeting nanoparticles based on hyaluronic and folic acids as a promising delivery system of the encapsulated 4-Methylumbelliferone (4-MU) against invasiveness of lung cancer in vivo and in vitro. *Int J Biol Macromol*. 2022;206:467–480. doi:10.1016/j.ijbiomac.2022.02.095
29. Qiu Z, Lu Z, Huang J, et al. Self-reinforced photodynamic immunostimulator to downregulate and block PD-L1 for metastatic breast cancer treatment. *Biomaterials*. 2023;303:122392. doi:10.1016/j.biomaterials.2023.122392
30. Terrones M, de Beeck KO, Van Camp G, Vandeweyer G, de Beeck KO. Pre-clinical modelling of ROS1+ non-small cell lung cancer. *Lung Cancer*. 2023;180:107192. doi:10.1016/j.lungcan.2023.107192
31. Brianna Lee SH, Lee SH. Chemotherapy: how to reduce its adverse effects while maintaining the potency? *Med Oncol*. 2023;40(3):88. doi:10.1007/s12032-023-01954-6
32. Feliu J, Heredia-Soto V, Gironés R, et al. Can we avoid the toxicity of chemotherapy in elderly cancer patients? *Crit Rev Oncol Hematol*. 2018;131:16–23. doi:10.1016/j.critrevonc.2018.08.008
33. Rohilla S, Dureja H, Chawla V. Cytoprotective agents to avoid chemotherapy induced sideeffects on normal cells: a review. *Curr Cancer Drug Targets*. 2019;19(10):765–781. doi:10.2174/1568009619666190326120457
34. DeRidder L, Robinson DA, Langer R, Traverso G. The past, present, and future of chemotherapy with a focus on individualization of drug dosing. *J Control Release*. 2022;352:840–860. doi:10.1016/j.jconrel.2022.10.043
35. Norouzi M, Hardy P. Clinical applications of nanomedicines in lung cancer treatment. *Acta Biomater*. 2021;121:134–142. doi:10.1016/j.actbio.2020.12.009
36. Ezhilarasan D, Lakshmi T, Mallineni SK. Nano-based targeted drug delivery for lung cancer: therapeutic avenues and challenges. *Nanomedicine*. 2022;17(24):1855–1869. doi:10.2217/nnm-2021-0364
37. Vikas Sahu HK, Mehata AK, Viswanadh MK, Priya V, Muthu MS, Muthu MS. Dual-receptor-targeted nanomedicines: emerging trends and advances in lung cancer therapeutics. *Nanomedicine*. 2022;17(19):1375–1395. doi:10.2217/nnm-2021-0470
38. de Lázaro I, Mooney DJ, de Lázaro I. Obstacles and opportunities in a forward vision for cancer nanomedicine. *Nat Mater*. 2021;20(11):1469–1479. doi:10.1038/s41563-021-01047-7
39. Cheng Z, Li M, Dey R, Chen Y. Nanomaterials for cancer therapy: current progress and perspectives. *J Hematol Oncol*. 2021;14(1):85. doi:10.1186/s13045-021-01096-0
40. Wang C, Li F, Zhang T, Yu M, Sun Y. Recent advances in anti-multidrug resistance for nano-drug delivery system. *Drug Deliv*. 2022;29(1):1684–1697. doi:10.1080/10717544.2022.2079771
41. Yang H, Shen W, Liu W, et al. PEGylated poly(α -lipoic acid) loaded with doxorubicin as a pH and reduction dual responsive nanomedicine for breast cancer therapy. *Biomacromolecules*. 2018;19(11):4492–4503. doi:10.1021/acs.biomac.8b01394
42. Wang K, Chen D, Zhang C, Lu L, Shang F, Li Y. Polyethylene glycol-modified cationic liposome as a promising nano spray for acute pneumonia treatment. *Polymers*. 2024;16(10):1384. doi:10.3390/polym16101384
43. Alassaif FR, Alassaif ER, Kaushik AK, Dhanapal J. Enhanced anti-proliferative effect of carboplatin in ovarian cancer cells exploiting chitosan-poly (lactic glycolic acid) nanoparticles. *Recent Pat Nanotechnol*. 2023;17(1):74–82. doi:10.2174/1872210516666220111160341
44. Włodarczyk MT, Dragulska SA, Chen Y, et al. Pt(II)-PLGA hybrid in a pH-responsive nanoparticle system targeting ovarian cancer. *Pharmaceutics*. 2023;15(2):607. doi:10.3390/pharmaceutics15020607
45. Zhu X, Yan S, Xiao F, Xue M. PLGA nanoparticles delivering CPT-11 combined with focused ultrasound inhibit platinum resistant ovarian cancer. *Transl Cancer Res*. 2021;10(4):1732–1743. doi:10.21037/tcr-20-3171
46. Paswan SK, Saini TR, Jahan S, Ganesh N. Designing and formulation optimization of hyaluronic acid conjugated PLGA nanoparticles of tamoxifen for tumor targeting. *Pharm Nanotechnol*. 2021;9(3):217–235. doi:10.2174/2211738509666210310155807

47. Iqbal H, Razzaq A, Khan NU, et al. pH-responsive albumin-coated biopolymeric nanoparticles with lapatinab for targeted breast cancer therapy. *Biomater Adv.* 2022;139:213039. doi:10.1016/j.bioadv.2022.213039
48. Male D, Gromnicova R. Nanocarriers for Delivery of Oligonucleotides to the CNS. *Int J mol Sci.* 2022;23(2):760. doi:10.3390/ijms23020760
49. Zaman MS, Chauhan N, Yallapu MM, et al. Curcumin nanoformulation for cervical cancer treatment. *Sci Rep.* 2016;6(1):20051. doi:10.1038/srep20051
50. Zhang ZT, Huang-Fu MY, Xu WH, Han M. Stimulus-responsive nanoscale delivery systems triggered by the enzymes in the tumor microenvironment. *Eur J Pharm Biopharm.* 2019;137:122–130. doi:10.1016/j.ejpb.2019.02.009
51. Jin X, Asghar S, Zhu X, et al. In vitro and in vivo evaluation of 10-hydroxycamptothecin-loaded poly (n-butyl cyanoacrylate) nanoparticles prepared by miniemulsion polymerization. *Colloids Surf B Biointerfaces.* 2018;162:25–34. doi:10.1016/j.colsurfb.2017.11.029
52. Tong X, Shi Z, Xu L, et al. Degradation behavior, cytotoxicity, hemolysis, and antibacterial properties of electro-deposited Zn-Cu metal foams as potential biodegradable bone implants. *Acta Biomater.* 2020;102:481–492. doi:10.1016/j.actbio.2019.11.031
53. Aoyama S, Motoori M, Yamasaki M, et al. The impact of weight loss during neoadjuvant chemotherapy on postoperative infectious complications and prognosis in patients with esophageal cancer: exploratory analysis of OGSG1003. *Esophagus.* 2023;20(2):225–233. doi:10.1007/s10388-022-00975-w
54. Xiong L, Lin XM, Nie JH, Ye HS, Liu J. Resveratrol and its nanoparticle suppress doxorubicin/docetaxel-resistant anaplastic thyroid cancer cells in vitro and in vivo. *Nanotheranostics.* 2021;5(2):143–154. doi:10.7150/ntno.53844

International Journal of Nanomedicine

Publish your work in this journal

The International Journal of Nanomedicine is an international, peer-reviewed journal focusing on the application of nanotechnology in diagnostics, therapeutics, and drug delivery systems throughout the biomedical field. This journal is indexed on PubMed Central, MedLine, CAS, SciSearch®, Current Contents®/Clinical Medicine, Journal Citation Reports/Science Edition, EMBase, Scopus and the Elsevier Bibliographic databases. The manuscript management system is completely online and includes a very quick and fair peer-review system, which is all easy to use. Visit <http://www.dovepress.com/testimonials.php> to read real quotes from published authors.

Submit your manuscript here: <https://www.dovepress.com/international-journal-of-nanomedicine-journal>

Dovepress
Taylor & Francis Group